JACS Au
AN OPEN ACCESS JOURNAL OF THE AMERICAN CHEMICAL SOCIETY

pubs.acs.org/jacsau Article

Organelle-Selective Membrane Labeling through Phospholipase D-Mediated Transphosphatidylation

Din-Chi Chiu and Jeremy M. Baskin*

Cite This: *JACS Au* 2022, 2, 2703−2713 Read Online

ACCESS | Metrics & More | Article Recommendations | Supporting Information

ABSTRACT: The specialized functions of eukaryotic organelles have motivated chemical approaches for their selective tagging and visualization. Here, we develop chemoenzymatic tools using metabolic labeling of abundant membrane lipids for selective visualization of organelle compartments. Synthetic choline analogues with three *N*-methyl substituents replaced with 2-azidoethyl and additional alkyl groups enabled the generation of corresponding derivatives of phosphatidylcholine (PC), a ubiquitous and abundant membrane phospholipid. Subsequent bioorthogonal tagging via the strain-promoted azide−alkyne cycloaddition (SPAAC) with a single cyclooctyne-fluorophore reagent enabled differential labeling of the endoplasmic reticulum, the Golgi complex, mitochondria, and lysosomes depending upon the substitution pattern at the choline ammonium center. Key to the success of this strategy was the harnessing of both the organic cation transporter OCT1 to enable cytosolic delivery of these cationic metabolic probes and endogenous phospholipase D enzymes for rapid, one-step metabolic conversion of the choline analogues to the desired lipid products. Detailed analysis of the trafficking kinetics of both the SPAAC-tagged fluorescent PC analogues and their non-fluorescent, azide-containing precursors revealed that the latter exhibit time-dependent differences in organelle selectivity, suggesting their use as probes for visualizing intracellular lipid transport pathways. By contrast, the stable localizations of the fluorescent PC analogues will allow applications not only for organelle-selective imaging but also for local modulation of physiological events with organelle-level precision by tethering of bioactive small molecules, via click chemistry, within defined subcellular membrane environments.

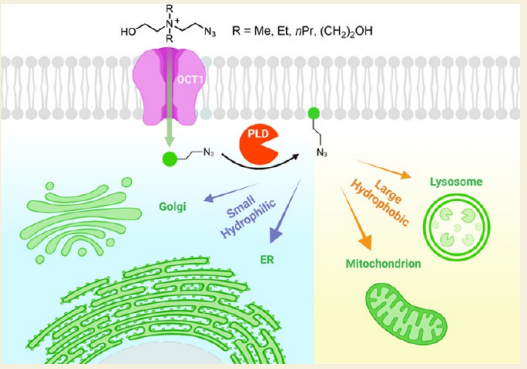

KEYWORDS: *bioorthogonal chemistry, click chemistry, lipids, membranes, phospholipids*

INTRODUCTION

Eukaryotic organelle membranes have unique lipid, protein, and glycan compositions that confer organelle identity and shape local physiological events. The specialization of organelle function and the dynamic nature of organelle homeostasis have inspired the development of fluorescent probes for selective visualization of different organelles in live cells. One approach involves expression of genetic fusions of fluorescent proteins with organelle-targeting peptides or domains, which—though widely used—requires transfection or genetic modification.[1−5] Alternatively, most organelles are targetable using small-molecule dyes with physicochemical properties that capitalize upon unique aspects of organelle biochemistry.[6] Several synthetic probes can label organelle lumens rather than their limiting membranes, and certain other synthetic organelle membrane-labeling probes can provide functional information by sensing local environmental changes such as mechanical forces,[7] polarity,[8] and pH.[9] However, as most of these probes are based on artificial rather than biomimetic scaffolds, they are less well suited to measuring dynamic aspects of organelle interplay, including inter-organelle membrane contact sites and intracellular lipid transport.

Instead, a different strategy involves covalent tagging of abundant lipid constituents of membranes using metabolic labeling and bioorthogonal chemistry.[10,11] Notably, phosphatidylcholine (PC) is an attractive target because it is the most abundant molecule in eukaryotic membranes.[12,13] Indeed, metabolic labeling of PC was first achieved using propargylcholine, an alkynyl analogue of choline, which is biosynthetically converted to PC via the multistep Kennedy pathway.[14,15] Propargylcholine labeling produces alkynyl PC, which can be visualized in fixed cells by Cu-catalyzed azide−alkyne cycloaddition (CuAAC) tagging with azide-bearing fluorophores.[16] For live-cell imaging, fluorescent PC derivatives can be generated by metabolic labeling with an azidocholine analogue (**1**, Figure 1A) followed by strain-promoted azide−alkyne cycloaddition (SPAAC) tagging with cyclooctyne-fluoro-

Received: July 28, 2022
Revised: October 30, 2022
Accepted: November 14, 2022
Published: November 28, 2022

ACS Publications
© 2022 The Authors. Published by American Chemical Society

https://doi.org/10.1021/jacsau.2c00419
JACS Au 2022, 2, 2703−2713

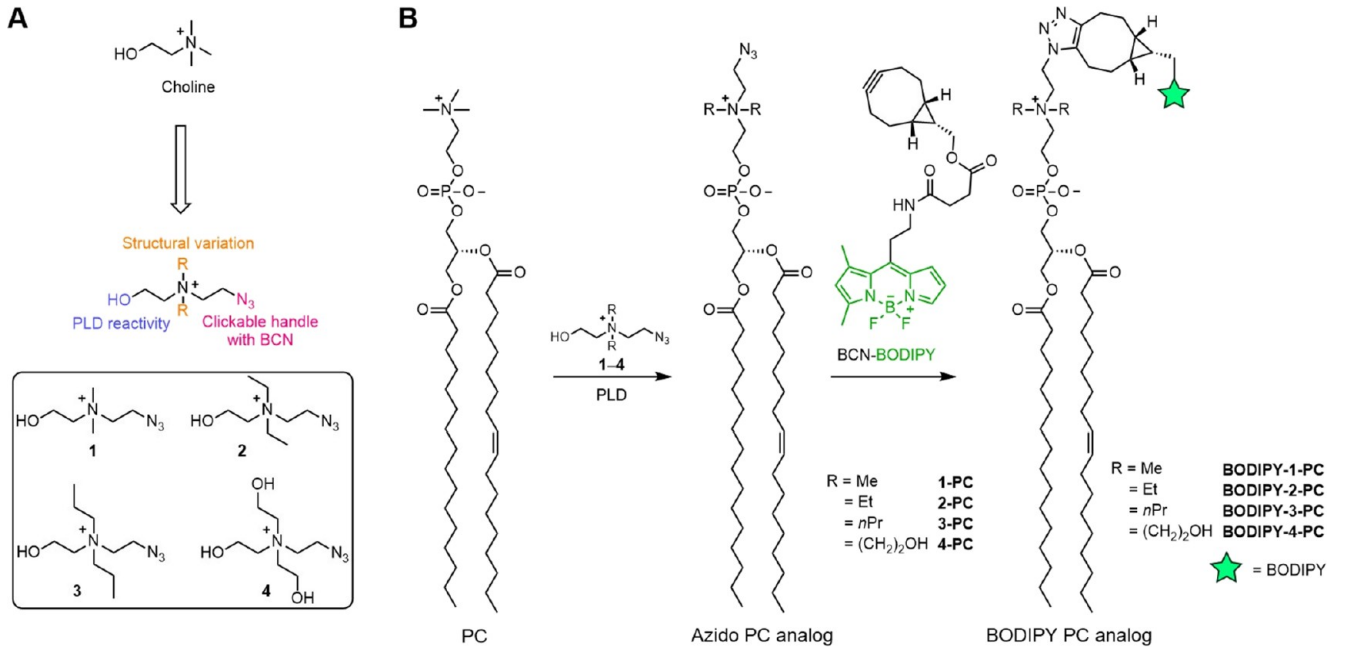

Figure 1. Design and use of azidocholine analogues for fluorescent tagging of organelle membranes using phospholipase D (PLD) activity. (A) Structures of bioorthogonal choline analogues bearing a 2-azidoethyl group (**1**) and replacement of two additional *N*-methyl groups in **1** with ethyl (**2**), *n*-propyl (**3**), and 2-hydroxyethyl (**4**). (B) Generation of fluorescent, bioorthogonal PC analogues in cells by IMPACT using transphosphatidylation of PC with **1**–**4** by PLDs, followed by SPAAC tagging with a cyclooctyne-fluorophore conjugate (BCN-BODIPY).

Table 1. LC–MS Characterization of 1-PC–4-PC Produced by PMA Stimulation[a]

				observed *m*/z [integration area (×10^5)]	
lipid	calculated mass[b]	t_R (min)[c]	FIPI	HeLa-WT	HeLa-hOCT1
1-PC	815.6021	6.2	–	815.6035 (11.8)	815.6040 (17.8)
			+	815.6002 (0.450)[d]	815.6000 (0.169)[d]
2-PC	843.6334	5.3	–	N.D.[e]	843.6281 (7.76)
			+	N.D.[e]	N.D.[e]
3-PC[f]	927.6909	5.5	–	N.D.[e]	927.6856 (0.871)
			+	N.D.[e]	N.D.[e]
4-PC	875.6234	5.7	–	N.D.[e]	875.6176 (1.27)
			+	N.D.[e]	N.D.[e]

[a]HeLa cells were incubated in a solution of a choline analogue (**1**–**4**, 1 mM) and PMA (100 nM) for 20 min in the absence or presence of the PLD inhibitor 5-fluoro-2-indolyl des-chlorohalopemide (FIPI) (750 nM). Lipids from the resulting cell lysates were extracted and analyzed by LC–MS to quantify the formation of the lipids of interest. [b]Calculated masses correspond to (34:1)-phospholipids. [c]Retention times (t_R) match those of a synthetic standard made in vitro using PLD from *Streptomyces sp.* PMF. [d]Minor PLD-independent labeling attributed to de novo PC biosynthesis[17] via the Kennedy pathway. [e]Not detected. [f]Because of interference from endogenous compounds with similar retention time, the identity of this lipid was determined following CuAAC derivatization with 2-propyn-1-ol.

phores.[17] Because PC is ubiquitous and abundant, this approach labels essentially all organelle membranes.

A recent strategy harnessed **1** for selective staining of organelle membranes including the endoplasmic reticulum (ER), Golgi complex, mitochondria, and lysosomes, wherein **1** was incorporated globally via the Kennedy pathway but the targeting selectivity was enabled by bespoke cyclooctyne reagents endowed with organelle-targeting groups that restricted the SPAAC reaction to the target organelles defined by the biased localization of the cyclooctyne reagent.[18] Though highly useful,[15] this modular approach required a different cyclooctyne reagent for each organelle and thus involved non-trivial synthetic efforts to produce the panel of detection reagents. In addition, although this approach enabled visualization of inter-organelle phospholipid transfer, the lipids carried bulky fluorophore tags that could potentially interfere with translocation rates and directions of transport.

We sought to devise an alternative, complementary strategy wherein organelle selectivity might be conferred by subtly structurally distinct choline analogues that could be introduced via a single rapid metabolic labeling step. We envisioned that the resultant lipid analogues would represent minimal perturbations relative to the natural lipid but that their differential trafficking behavior and localization could be subsequently visualized following a bioorthogonal tagging reaction to introduce a fluorescent label. Therefore, we designed and synthesized a panel of azidocholine analogues with different sizes and hydrophilicities by replacement of the *N*-methyl substituents with various alkyl groups (**2**–**4**, Figure 1A). We hypothesized that, if these probes could be incorporated into the corresponding PC analogues, their different physicochemical properties might endow these bioorthogonal lipids with distinct trafficking properties and organelle membrane affinities, enabling a versatile organelle-

https://doi.org/10.1021/jacsau.2c00419
JACS Au 2022, 2, 2703–2713

selective imaging strategy using a single cyclooctyne-fluorophore reagent.

RESULTS AND DISCUSSION

OCT1-Assisted Metabolic Incorporation of Bioorthogonal Choline Analogues

We synthesized **2**−**4** (Figure 1A) analogously to a published route for **1** in 1−2 steps and 75−83% overall yields (Scheme S1).[17] To evaluate the ability of **2**−**4** to be incorporated into the corresponding PC analogues, we elected to bypass the multistep and slow Kennedy pathway by taking advantage of phospholipase D (PLD) enzymes, which we recently showed can catalyze PC transphosphatidylation with propargylcholine to produce alkynyl PC.[19] Indeed, treatment of HeLa cells with **1** and stimulation of endogenous PLDs with the protein kinase C (PKC) agonist phorbol 12-myristate 13-acetate (PMA) formed the azido PC analogue **1-PC**, detected by LC−MS (Table 1).

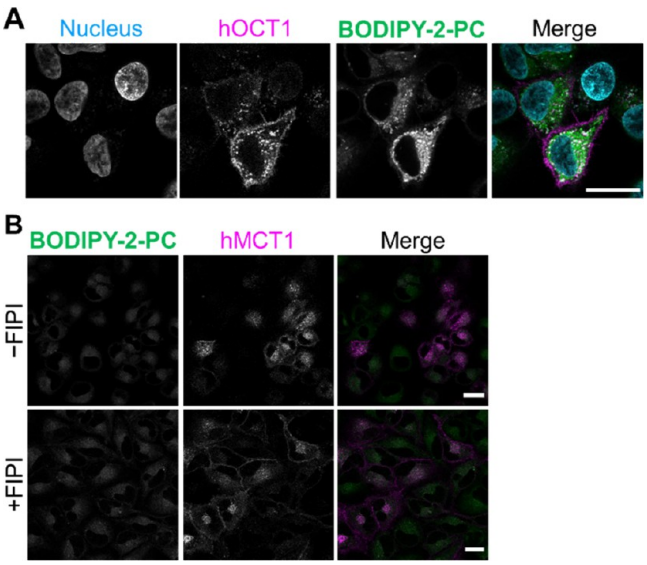

Figure 2. IMPACT labeling of HeLa cells with choline analogue **2** requires hOCT1 expression. (A) Wildtype HeLa cells were transiently transfected with hOCT1-miRFP and then labeled via IMPACT with **2** and PMA stimulation followed by SPAAC tagging with BCN-BODIPY. Note that IMPACT labeling intensity correlates with hOCT1-miRFP expression levels. (B) Transfection of HeLa cells with hMCT1-mCherry did not facilitate IMPACT labeling with **2**. HeLa cells were transiently transfected with hMCT1-mCherry and then labeled via IMPACT with **2** and PMA stimulation, in the absence or presence of the pan-PLD inhibitor FIPI, followed by SPAAC tagging with BCN-BODIPY. Scale bars: 20 μm.

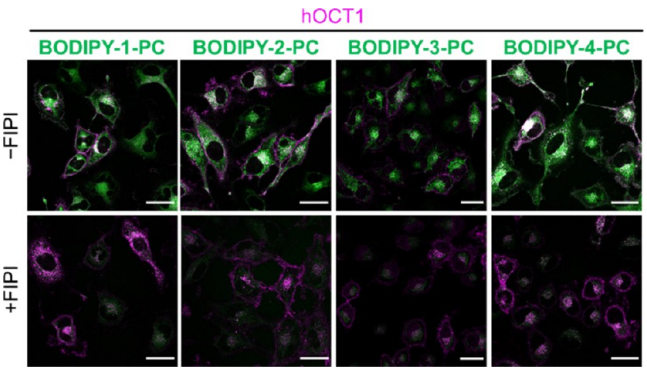

Figure 3. Stable expression of hOCT1 enables uniform IMPACT labeling of lipids derived from **1**−**4**. HeLa-hOCT1 cells were labeled with **1**−**4** (1 mM) and PMA (100 nM) for 10 min with FIPI (750 nM) or vehicle (except for **3**, whose 5-min labeling with PMA was preceded a 10-min PMA pre-incubation; see Figure S5). Cells were then tagged via SPAAC with BCN-BODIPY (1 μM) and imaged by confocal microscopy. Scale bars: 30 μm.

However, similar experiments with **2**−**4** yielded no detectable formation of **2-PC**, **3-PC**, or **4-PC**. Given the wide primary alcohol substrate tolerance of PLDs for transphosphatidylation,[20] we posited that wildtype HeLa cells failed to import **2**−**4**, which are bulky, cationic, and more structurally divergent from choline than **1**, which is likely a substrate for endogenous choline transporters. To overcome this obstacle, we hypothesized that the ectopic expression of a more promiscuous transporter might enable the import of **2**−**4**. We identified organic cation transporter 1 (OCT1/SLC22A1), a member of the solute carrier (SLC) superfamily, as a promising candidate, due to its broad substrate scope toward small organic cationic cargos and tolerance to PKC activation, which we have employed to activate PLDs.[21−24] Thus, we cloned an infrared fluorescent protein fusion to human OCT1 (hOCT1-miRFP).

Transfection of HeLa cells with hOCT1-miRFP resulted in successful metabolic labeling with **2** in the presence of PMA stimulation, as observed by confocal microscopy following SPAAC tagging with BCN−BODIPY,[25] a procedure we have termed Imaging Phospholipase D Activity with Clickable Alcohols via Transphosphatidylation (IMPACT, Figures 1B and 2A).[26,27] These data indicate that hOCT1 expression is required for the import of **2**. As a control, we expressed in HeLa cells another SLC superfamily member known to transport different types of metabolites (the human monocarboxylate transporter 1 MCT1/SLC16A1), which is not expected to transport positively charged compounds, and we found that MCT1 did not enable IMPACT labeling with choline analogue **2** (Figure 2B).

Transient expression of hOCT1 clearly enabled the incorporation of *N*,*N*-diethyl-containing probe **2**. Because the labeling intensity correlated with hOCT1 levels (Figure 2A), we envisioned creating a stable cell line exhibiting uniform hOCT1 expression levels to enable more consistent labeling for quantitative analyses. Therefore, we generated a stable HeLa cell line expressing hOCT1 (HeLa-hOCT1) using lentiviral delivery and FACS sorting (Figure S1).[28] Gratifyingly, treatment of HeLa-hOCT1 cells with **1**−**4** and stimulation of PLD activity using PMA led to the formation of the corresponding azido lipids, as determined by LC−MS analysis of cell lysates (**1-PC**−**4-PC**) (Table 1 and Figure S2). Importantly, treatment with the pan-PLD inhibitor FIPI during the alcohol labeling step prevented the formation of the PC analogues, indicating the requirement for PLD activity to produce the labeled lipids.[29] Further, to investigate the stability of our PC derivatives, we incubated cells post-transphosphatidylation for 3 h and examined lipid extracts by LC−MS. These studies revealed that levels of **1-PC**, **2-PC**, and **3-PC** did not decrease over this interval (Figure S3), establishing that PC analogues generated from **1**−**3** are stable and trackable intermediates.

To support the LC−MS results, we analyzed azido lipids **1-PC**−**3-PC** by labeling HeLa-hOCT1 cells with **1**−**3** under conditions of PLD stimulation followed by lipid extraction and

https://doi.org/10.1021/jacsau.2c00419
JACS Au 2022, 2, 2703−2713

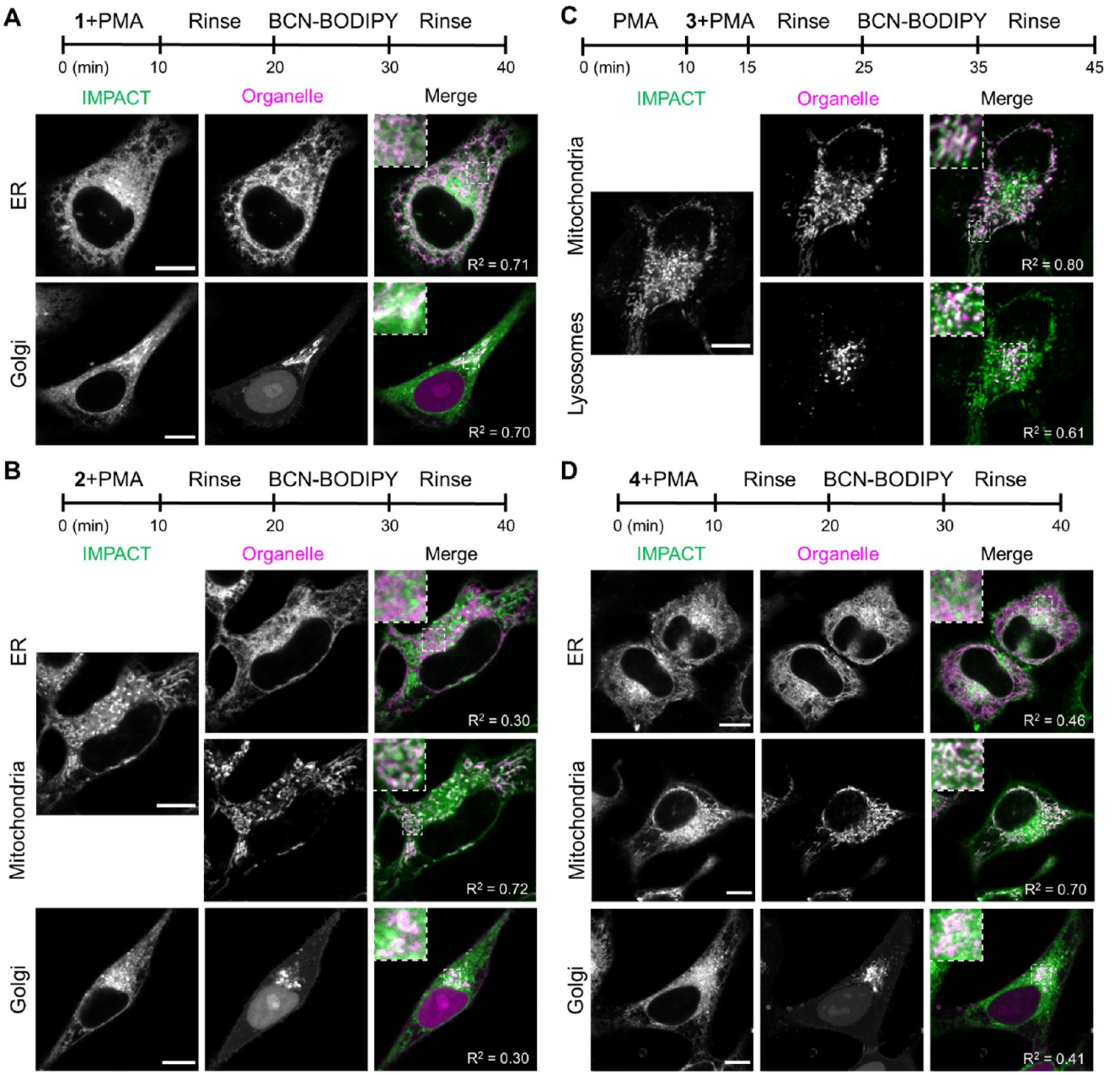

Figure 4. Colocalization analysis reveals different subcellular localizations for BODIPY-tagged PC analogues derived from **1**−**4**. The colocalization analysis of IMPACT (green) in HeLa-hOCT1 cells labeled with **1** (A), **2** (B), **3** (C), and **4** (D) expressing or labeled with markers for these organelles (magenta): ER (STIM1-mRFP); Golgi [mCherry-PH(OSBP)], mitochondria (MitoView 405), and lysosomes (LysoTracker Red DND-99). The labeling protocol is shown above each set of images. Merged images show the colocalization of IMPACT (green) with a single organelle marker. In B and C, note that some cells [ER/mitochondria in (B) and mitochondria/lysosomes in (C)] were labeled with three different reagents (i.e., IMPACT and organelle markers in both blue and red), and each merged image shows IMPACT and only one of the organelle markers. Pearson's correlation coefficients (R^2) between IMPACT and the organelle marker are indicated in each image. See also Figure S6. Scale bars: 10 μm.

SPAAC tagging in vitro with BCN-BODIPY to obtain BODIPY-tagged PC analogues that were subsequently characterized by HPLC. We observed peaks corresponding to **BODIPY-1-PC**−**BODIPY-3-PC** whose presence was sensitive to FIPI treatment (Figure S4), indicating that they were the products of PLD-mediated transphosphatidylation. Interestingly, **BODIPY-4-PC**, which has two additional free hydroxyl groups, could not be reliably characterized by this HPLC analysis, owing to presumed degradation during the overnight (42 °C) SPAAC reaction in vitro.

OCT1 is a member of the SLC superfamily of metabolite, ion, and peptide transporters, many members of which impact drug metabolism, and pharmacokinetics, and more broadly play key roles in metabolism and physiology.[30−32] To our knowledge, no SLC transporter has been exploited in a chemical biology context to assist in the cellular uptake of otherwise impermeable metabolic labeling probes. Our repurposing of hOCT1 not only surmounts the permeability issue of unnatural choline analogues, but, more generally, we propose that OCT1 and other SLC superfamily transporters

https://doi.org/10.1021/jacsau.2c00419
JACS Au 2022, 2, 2703−2713

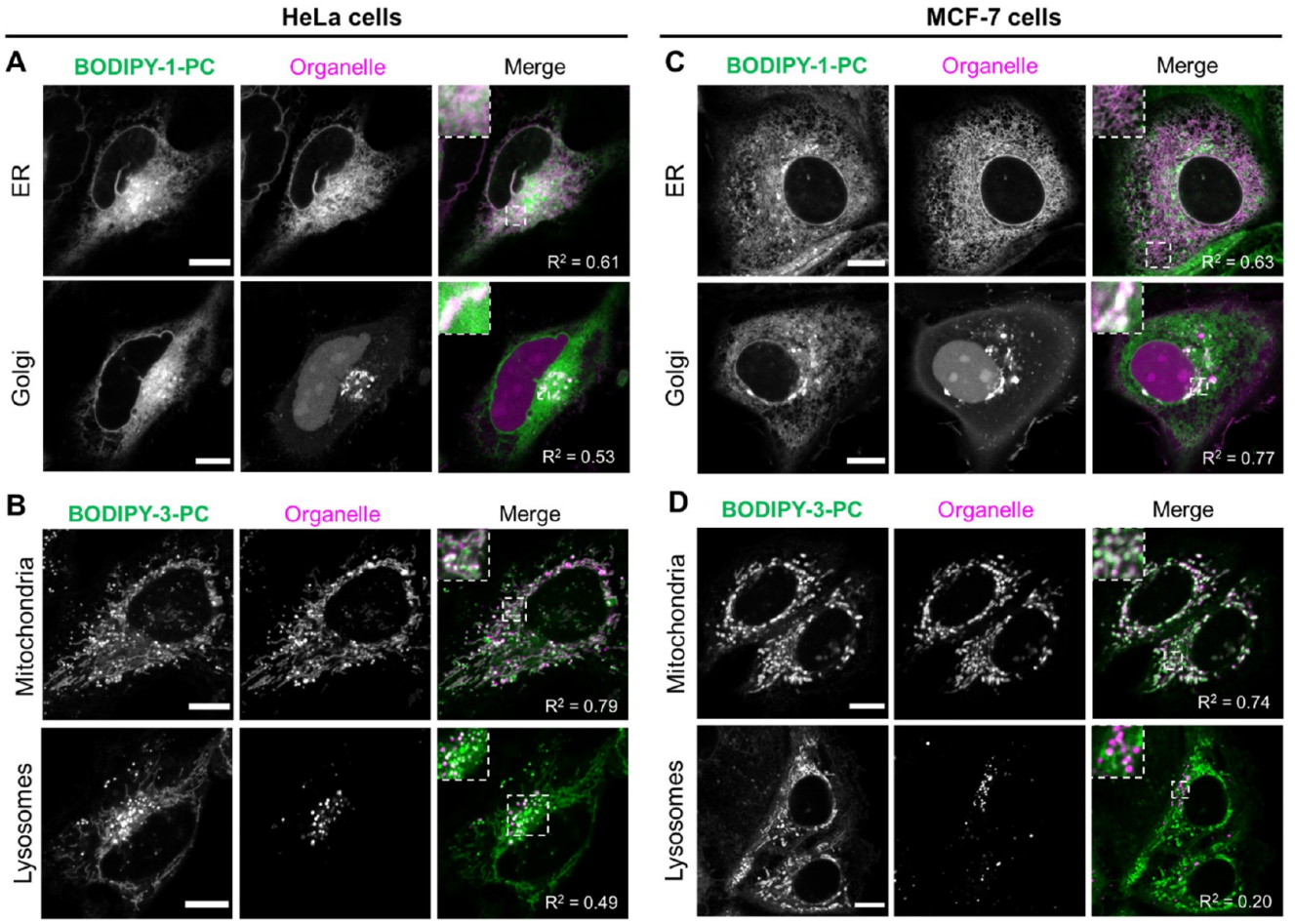

Figure 5. Organelle-selective tagging with different choline analogues is generalizable to transient transfection in two different cell lines. Colocalization analysis of IMPACT (green) in hOCT1-transfected HeLa (A–B) or MCF-7 (C–D) cells labeled in the presence of PMA with **1** (A and C) or **3** (B and D). Cells were also transiently transfected or labeled with markers for these organelles (magenta): ER (Sec61β-mRFP); Golgi [mCherry-PH(OSBP)], mitochondria (MitoView 405), and lysosomes (LysoTracker Red DND-99). Pearson's correlation coefficients (R^2) between IMPACT and the organelle marker are indicated in each image. See also Figure S7. Scale bars: 10 μm.

could serve as valuable tools to resolve a key challenge in chemical biology, that of cell-impermeability of hydrophilic chemical probes.

Intracellular Localization of BODIPY-PC Analogues

To assess the subcellular localization of the bioorthogonal PC analogues, we labeled HeLa-hOCT1 cells with **1**–**4** via IMPACT (Figure 1B). Fluorescence labeling was only observed in the samples lacking FIPI, confirming the requirement for PLD activity (Figure 3). Whereas **1**, **2**, and **4** were all rinsed out rapidly prior to SPAAC tagging, a shorter labeling period during maximal PLD activity was necessary to minimize undesired PLD-independent background in cells labeled with **3** (Figures 3 and S5).

Upon inspection of the intracellular distributions of the BODIPY-tagged PC analogues, we observed different subcellular localizations, prompting us to perform detailed colocalization analysis with organelle markers (Figures 4 and S6). **BODIPY-1-PC** exhibited strong colocalization with ER and Golgi complex markers (Figure 4A) and little overlap with mitochondrial, lysosomal, and plasma membrane markers (Figure S6A). By contrast, even though **BODIPY-2-PC** only differs from **BODIPY-1-PC** by elongation of two *N*-methyl to *N*-ethyl groups, it colocalized substantially less with ER and Golgi markers, instead colocalizing strongly with a mitochondrial marker (Figure 4B) and moderately with a lysosomal marker (Figure S6B). Further elongation to *N*-propyl groups, as in **BODIPY-3-PC**, led to highly selective mitochondrial and lysosomal labeling (Figure 4C), with virtually complete loss of ER and Golgi labeling (Figure S6C). Finally, **BODIPY-4-PC**, which is similar in size to **BODIPY-3-PC** but more hydrophilic, localized predominantly to mitochondria (Figure 4D), with minor pools at the ER and Golgi (Figure 4D) and, interestingly, the plasma membrane (Figure S6D) but minimal localization to lysosomes (Figure S6D). Similarly, wildtype HeLa cells transiently transfected with hOCT1-miRFP and labeled with analogues **1** (Figures 5A and S7A) or **3** (Figures 5B and S7B) exhibited identical organelle selectivities as in the stable HeLa-hOCT1 cell line, that is, ER and Golgi preference for **1** and mitochondria and lysosome preference for **3**, highlighting the suitability of our approach to scenarios where transient transfection is preferred.

To assess the generality of this method, wildtype MCF-7 cells transiently transfected with hOCT1-miRFP were subjected to IMPACT labeling with choline analogues **1** (Figures 5C and S7C) and **3** (Figures 5D and S7D) in the absence or presence of FIPI (Figure S7E). As in HeLa cells, we found that MCF-7 cells exhibited OCT1-independent labeling with **1** but required OCT1 expression to enable labeling with

https://doi.org/10.1021/jacsau.2c00419
JACS Au 2022, 2, 2703–2713

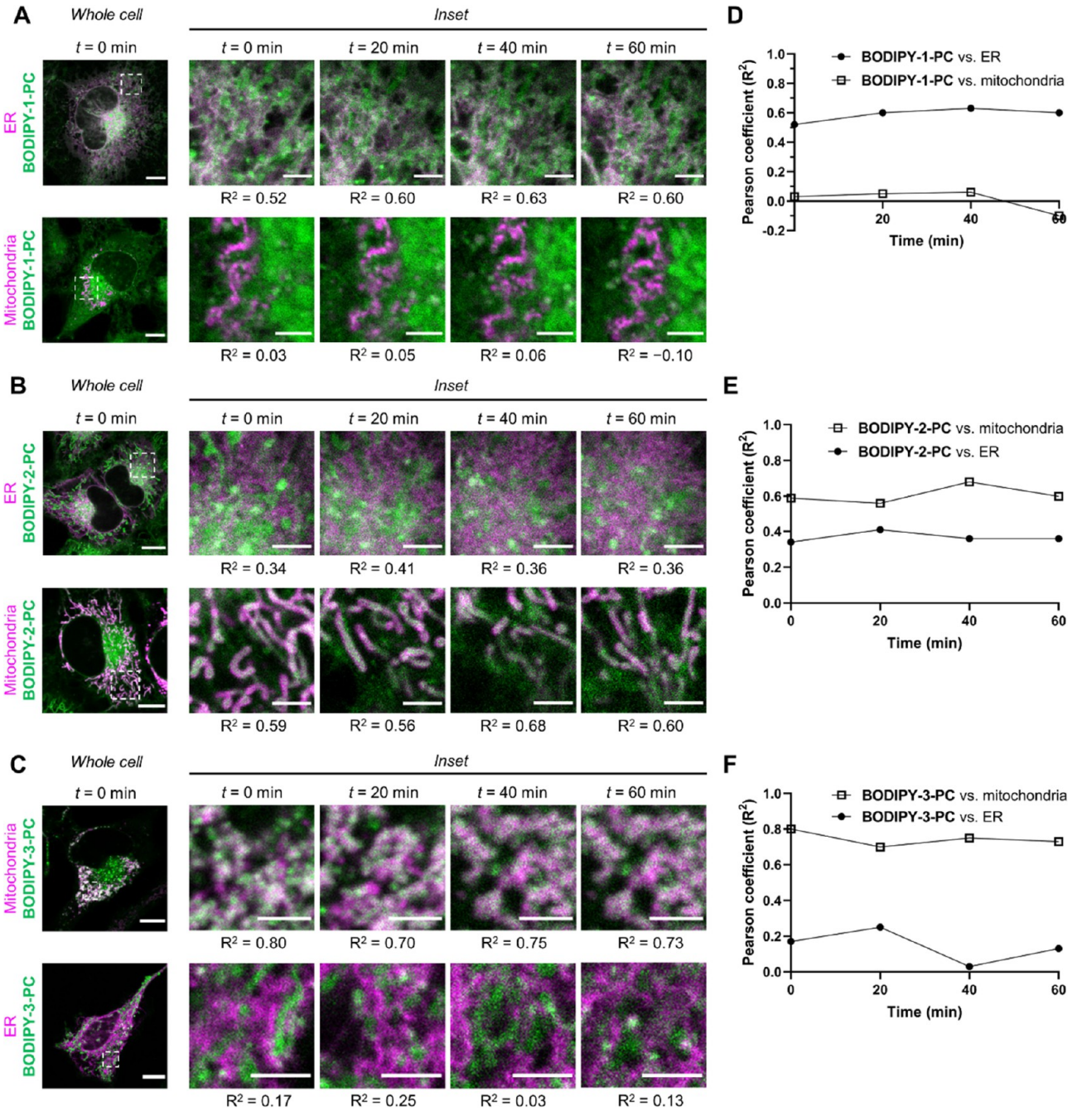

Figure 6. Subcellular localizations of BODIPY-tagged PC analogues derived from **1**−**3** are stable over 1 h. Colocalization analyses of **BODIPY-1-PC** (A), **BODIPY-2-PC** (B), and **BODIPY-3-PC** (C) generated by IMPACT in HeLa-hOCT1 cells expressing markers for the ER (Sec61β-mRFP) and mitochondria (OMP25TM-mCherry) and monitored for the subsequent hour, with plots of Pearson's correlation coefficients (R^2) of IMPACT with ER or mitochondrial markers over time for **BODIPY-1-PC** (D), **BODIPY-2-PC** (E), and **BODIPY-3-PC** (F). Scale bars: 10 μm (whole cells) and 3 μm (insets).

3. The subcellular localization pattern of **BODIPY-1-PC** in MCF-7 cells was similar to that in HeLa cells, where most of the signal emanated from the ER and Golgi. Further, **BODIPY-3-PC** was localized to mitochondria but not ER and Golgi in MCF-7 cells, as in HeLa cells. However, this lipid was not observed in lysosomes in MCF-7 cells. This interesting observation reveals an example of single organelle labeling by our method, which may be a result of the differences in lipid trafficking pathway activities in different cell lines.

Dynamic Trafficking Behavior of BODIPY-PC Analogues

The colocalization data from HeLa and MCF-7 cells revealed a striking trend, wherein elongation of the *N*-alkyl substituent in **1**−**3** increased the propensity of the resultant BODIPY-tagged PC analogue to adopt mitochondrial rather than ER/Golgi localizations. Because PLD-derived bioorthogonal lipids generated during PMA stimulation are most likely synthesized at the plasma membrane,[33,34] we hypothesized that inter-organelle lipid transport pathways may contribute to establishing the localizations of these lipids, motivating us to investigate the stability of the labeling over time.[35−38] We note, however,

https://doi.org/10.1021/jacsau.2c00419
JACS Au 2022, 2, 2703−2713

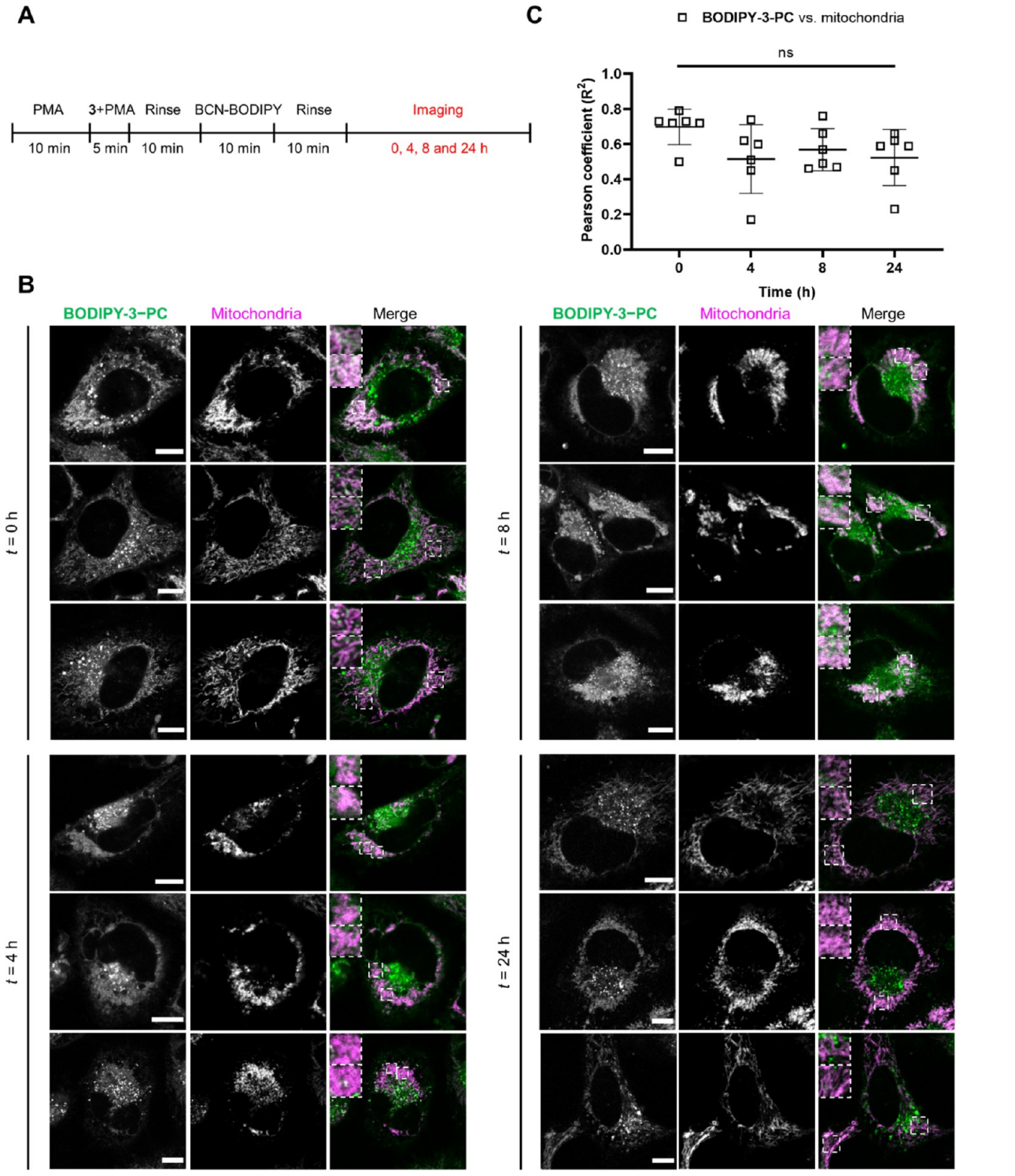

Figure 7. Subcellular localization of **BODIPY-3-PC** to mitochondria is stable over 24 h. Colocalization analysis of **BODIPY-3-PC** generated by IMPACT [procedure shown in (A)] in HeLa-hOCT1 cells expressing a mitochondrial marker (OMP25TM-mCherry) and monitored over the subsequent 24 h (B). Pearson's correlation coefficients (R^2) between IMPACT and the organelle marker vs post-IMPACT time are plotted in (C). Scale bars: 10 μm. ANOVA (two-way): ns, not significant (n = 6 areas from 3 cells).

that mitochondrial PLD activity has been proposed, by both PLD6 and, recently, PLD2, and the latter of these is capable of transphosphatidylation, suggesting that transphosphatidylation of **3** may occur directly on mitochondrial membranes.[26,39−41]

By monitoring the colocalization of **BODIPY-1-PC**, **BODIPY-2-PC**, and **BODIPY-3-PC** over 1 h with ER and mitochondrial markers, we found that **BODIPY-1-PC** retained its ER but not mitochondrial localization (Figure 6A,D), whereas **BODIPY-3-PC** conversely retained its mitochondrial but not ER localization (Figure 6C,F). **BODIPY-2-PC** exhibited an intermediate but stable phenotype, with partial colocalization with both markers (Figure 6B,E). These time series studies suggest that the BODIPY-PC analogues are stable for at least an hour.

https://doi.org/10.1021/jacsau.2c00419
JACS Au 2022, 2, 2703−2713

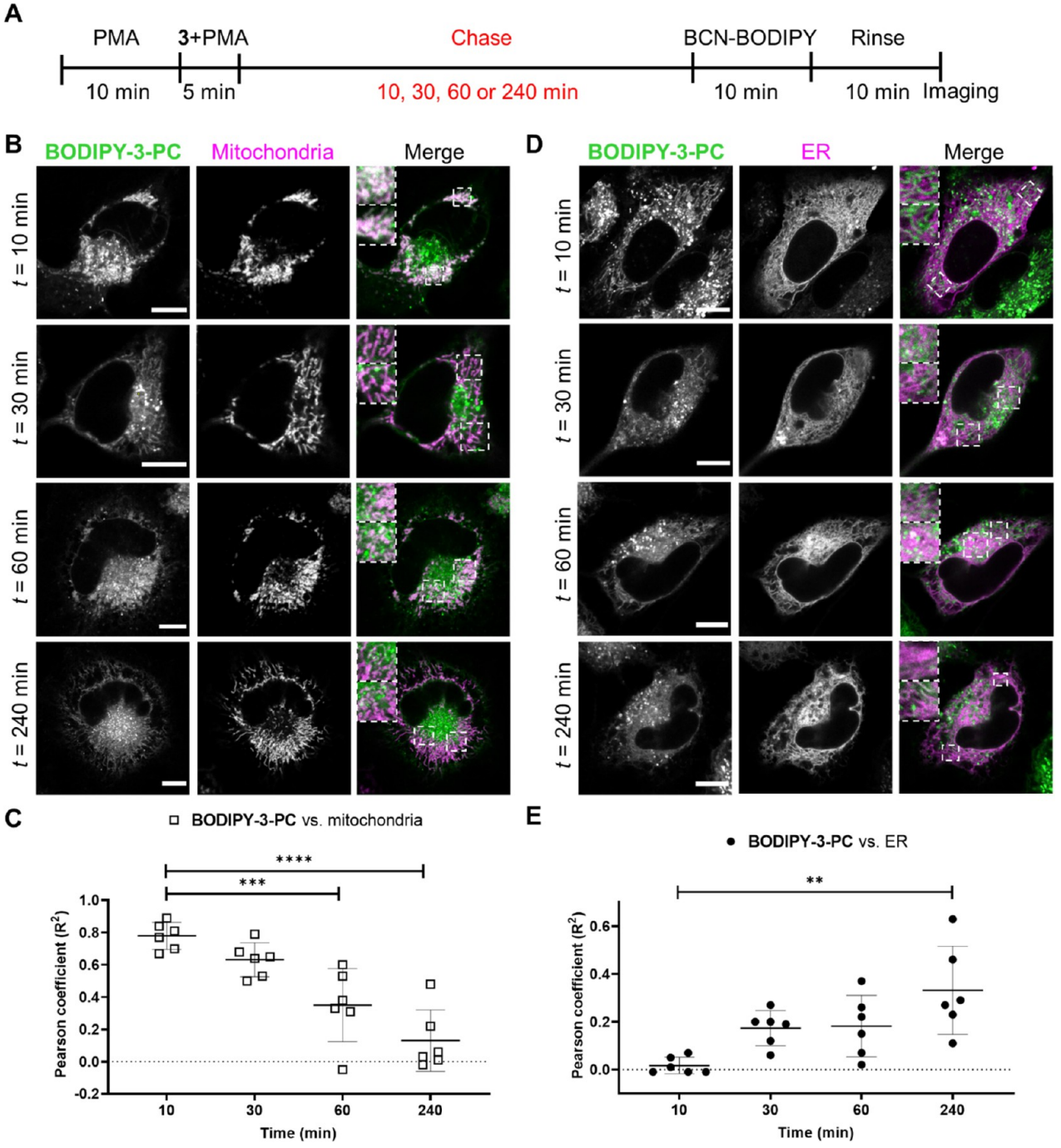

Figure 8. Pulse-chase labeling reveals dynamic trafficking of non-fluorescent, azido PC analogues derived from **3**. Colocalization analysis of **BODIPY-3-PC** generated by IMPACT with varied post-transphosphatidylation chase times, as illustrated in (A), in HeLa-hOCT1 cells expressing markers for mitochondria [OMP25TM-mCherry, (B)] or ER [Sec61β-mRFP, (D)]. Changes over time in the colocalization of **BODIPY-3-PC** with either mitochondrial (C) or ER (E) markers were quantified by determination and plotting of Pearson's coefficients (R^2). Scale bars: 10 μm. ANOVA (two-way): $^{**}p < 0.01$, $^{***}p < 0.001$, and $^{****}p < 0.0001$ (n = 6 areas from 3 cells).

We next performed longer time-course experiments to assess the long-term trafficking of our BODIPY-PC analogues Figures 7a and (S8A). Although much of the area labeled by **BODIPY-1-PC** remained colocalized with the ER for 4 h after SPAAC tagging, we did observe the formation of puncta that did not reside on the ER, and further incubation until 24 h post-SPAAC led to complete loss of the ER localization of **BODIPY-1-PC** (Figure S8B,C), which is consistent with previous observations that fluorophore-tagged **1-PC** is eventually transferred to other organelles over time post-SPAAC.[18] Interestingly, **BODIPY-3-PC** did not exhibit a similar tendency of intracellular migration. Over the course of a 24-h incubation post-SPAAC (Figure 7A), **BODIPY-3-PC** was strikingly persistent on mitochondria (Figure 7B,C), which implies the lack of a transfer mechanism for **BODIPY-3-PC** from mitochondria to other organelle membranes and highlights its utility for long-term labeling of mitochondrial membranes.

https://doi.org/10.1021/jacsau.2c00419
JACS Au 2022, 2, 2703−2713

Intracellular Trafficking of Non-fluorescent, Azido PC Analogues

The monitoring of bioorthogonal lipid analogues tagged by a fluorophore is a widely applied strategy to study the localizations and intracellular transport of lipids. However, such methodologies have the inherent drawback that the attachment of a large fluorophore unit to the lipid can change the biophysical and biochemical properties of the resultant lipid analogue, leading to behavior that can be much different from the native lipid. By contrast, the azido lipid analogues generated in our approach are produced and potentially trafficked to the desired organelle membranes before being labeled with the much larger fluorophore tag. Therefore, we envisioned that by incorporating a variable chase time in between PLD transphosphatidylation and SPAAC tagging, we would be able to visualize the intracellular, inter-organelle transfer of these non-fluorescent, azido lipids, whose structures more closely resemble native PC.

Thus, we adapted our procedure to incorporate a range of chase times (from 10 min to 4 h post-transphosphatidylation), followed by SPAAC tagging with BCN-BODIPY and imaging by confocal microscopy, to assess trafficking of the azido PC analogues (Figure 8A). We first focused on **3-PC**, which was detected on mitochondria when PLD transphosphatidylation was immediately followed by SPAAC tagging (e.g., Figure 4C). However, the introduction of a post-transphosphatidylation chase of up to 4 h revealed migration of the lipid from mitochondria to other organelles, including notably the ER. Over this 4-h chase time, the colocalization of IMPACT with a mitochondrial marker steadily dropped (Figure 8B,C), whereas the colocalization of IMPACT with an ER marker steadily increased (Figure 8D,E). The observed inter-organelle transport of **3-PC** stands in contrast to the persistent mitochondrial labeling of **BODIPY-3-PC** over 24 h (Figure 7).

Conversely, the ER localization of **BODIPY-1-PC** did not significantly change with longer post-transphosphatidylation chase times (Figure S9), which also differs from the observed changes to the intracellular distribution of **BODIPY-1-PC** over time (Figure S8). Overall, the observations from these pulse-chase experiments highlight the influence of the differing effects of the chemical modifications to PC analogues on the trafficking of these bioorthogonal lipids.

Putting together the results of the comparative studies using labeling with **1** and **3**, azido analogues **1-PC** and **3-PC** accumulate in the ER over time, regardless of their initial localization. However, BODIPY tagging of azido PC analogues in the mitochondria results in their sequestration there, whereas azido lipids that are fluorescently tagged in the ER or Golgi complex are ultimately trafficked to lysosomes.

CONCLUSIONS

We developed a series of bioorthogonal choline analogues with increasing steric bulk at the ammonium center that are processed by the cellular machinery to yield stable metabolic labeling of unique organelle membranes and in some cases can report on inter-organelle lipid transport pathways. Key to this advance was the discovery that the heterologous expression of OCT1 enables the cellular import of cationic choline analogues, suggesting its use for cytosolic delivery of small cationic cargoes and potentially the use of other SLC transporters for the import of other types of cell-impermeable probes. The PC analogues generated from **1**−**4** via PLD transphosphatidylation adopted different subcellular localizations and exhibited different intracellular transport behavior. Analogues closer in structure to natural PC were predominantly ER- and Golgi-localized, whereas those with longer *N*-alkyl chains preferentially accumulated in mitochondria. Interestingly, the mechanisms underlying the observed differential localizations of the PC analogues produced by PLD transphosphatidylation of **1**−**4** remain unknown. We posit that they are likely the result of a combination of the following factors: differences in localizations of soluble probes **1**−**4**; different affinities of the bioorthogonal PC analogues for the lipid transfer proteins, scramblases, and flippases that mediate inter-organelle lipid trafficking; and different affinities of PC analogues for certain organelle membrane environments.

One useful application of the organelle-targeting propensities of our probes is monitoring of the trafficking of not only the BODIPY-functionalized PC analogues but also, via pulse-chase experiments, the minimally perturbing azido PC analogues. For example, **3-PC** was initially localized on mitochondria, but it was capable of being transported from mitochondria to the ER, whereas **1-PC** continued to reside on ER membranes even after a prolonged chase. These localizations and trafficking patterns differed from the BODIPY-tagged PC analogues, however, as **BODIPY-3-PC** exhibited a stable mitochondrial localization, suggesting that BODIPY-tagged lipids are trafficked differently than the azido analogues and highlighting the importance of developing minimalist tags for studying inter-organelle lipid transfer pathways.

Because choline analogues **1**−**4** enable azide incorporation into abundant lipids on defined organelle subsets, and functionalized lipids **BODIPY-1-PC** and **BODIPY-3-PC** exhibit spatial stability for several hours, we envision the use of these probes not only for organelle-selective imaging and monitoring of inter-organelle lipid transport but also, potentially, local modulation of physiological events with organelle-level precision by tethering of bioactive small molecules within defined subcellular membrane environments.

ASSOCIATED CONTENT

Supporting Information

The Supporting Information is available free of charge at https://pubs.acs.org/doi/10.1021/jacsau.2c00419.

Synthesis of choline analogues, generation of a HeLa cell line stably expressing hOCT1, characterization of **3-PC** by LC−MS, pulse-chase experiment to examine metabolic stability, HPLC analysis of BODIPY-tagged PC analogues, optimization of IMPACT labeling protocol with **3**, colocalization analysis of IMPACT labeling HeLa-hOCT1 cells, colocalization analysis of IMPACT labeling with organelle markers, the fluorescent PC analogue **BODIPY-1-PC**, the azido PC analogue **1-PC** stably localizes to the ER over 4 hours, materials and methods, 1H and 13C NMR spectra, and supporting information references (PDF)

AUTHOR INFORMATION

Corresponding Author

Jeremy M. Baskin − *Department of Chemistry and Chemical Biology, Cornell University, Ithaca, New York 14853, United States; Weill Institute for Cell and Molecular Biology, Cornell University, Ithaca, New York 14853, United States;*

https://doi.org/10.1021/jacsau.2c00419
JACS Au 2022, 2, 2703−2713

orcid.org/0000-0003-2939-3138;
Email: jeremy.baskin@cornell.edu

Author

Din-Chi Chiu − *Department of Chemistry and Chemical Biology, Cornell University, Ithaca, New York 14853, United States; Weill Institute for Cell and Molecular Biology, Cornell University, Ithaca, New York 14853, United States*

Complete contact information is available at: https://pubs.acs.org/10.1021/jacsau.2c00419

Author Contributions

D.-C.C. and J.M.B. designed experiments, analyzed results, and wrote the manuscript. D.-C.C. performed all experiments and data analysis. CRediT: **Din-Chi Chiu** conceptualization, formal analysis, investigation, writing-original draft, writing-review & editing; **Jeremy M. Baskin** conceptualization, formal analysis, funding acquisition, project administration, supervision, writing-original draft, writing-review & editing.

Notes

The authors declare no competing financial interest.

■ ACKNOWLEDGMENTS

We acknowledge support from the NSF (CAREER CHE-1749919), a Beckman Young Investigator Award, and a Sloan Research Fellowship. We thank Timothy Bumpus, Brittany White-Mathieu, and Reika Tei for reagents and technical assistance, and Brittany White-Mathieu for detailed edits and suggestions on the manuscript. This work made use of the Cornell University NMR Facility, which is supported in part by the NSF (CHE-1531632).

■ REFERENCES

(1) Chudakov, D. M.; Matz, M. V.; Lukyanov, S.; Lukyanov, K. A. Fluorescent Proteins and Their Applications in Imaging Living Cells and Tissues. *Physiol. Rev.* **2010**, *90*, 1103−1163.
(2) Snapp, E. Design and Use of Fluorescent Fusion Proteins in Cell Biology. *Curr. Protoc. Cell Biol.* **2005**, *27*, 21.4.1.
(3) Kimura, S.; Noda, T.; Yoshimori, T. Dissection of the Autophagosome Maturation Process by a Novel Reporter Protein, Tandem Fluorescent-Tagged LC3. *Autophagy* **2007**, *3*, 452−460.
(4) Pankiv, S.; Clausen, T. H.; Lamark, T.; Brech, A.; Bruun, J.-A.; Outzen, H.; Øvervatn, A.; Bjørkøy, G.; Johansen, T. P62/SQSTM1 Binds Directly to Atg8/LC3 to Facilitate Degradation of Ubiquitinated Protein Aggregates by Autophagy. *J. Biol. Chem.* **2007**, *282*, 24131−24145.
(5) Losev, E.; Reinke, C. A.; Jellen, J.; Strongin, D. E.; Bevis, B. J.; Glick, B. S. Golgi Maturation Visualized in Living Yeast. *Nature* **2006**, *441*, 1002−1006.
(6) Toyama, E. Q.; Herzig, S.; Courchet, J.; Lewis, T. L.; Losón, O. C.; Hellberg, K.; Young, N. P.; Chen, H.; Polleux, F.; Chan, D. C.; Shaw, R. J. AMP-Activated Protein Kinase Mediates Mitochondrial Fission in Response to Energy Stress. *Science* **2016**, *351*, 275−281.
(7) Goujon, A.; Colom, A.; Straková, K.; Mercier, V.; Mahecic, D.; Manley, S.; Sakai, N.; Roux, A.; Matile, S. Mechanosensitive Fluorescent Probes to Image Membrane Tension in Mitochondria, Endoplasmic Reticulum, and Lysosomes. *J. Am. Chem. Soc.* **2019**, *141*, 3380−3384.
(8) Danylchuk, D. I.; Jouard, P.-H.; Klymchenko, A. S. Targeted Solvatochromic Fluorescent Probes for Imaging Lipid Order in Organelles under Oxidative and Mechanical Stress. *J. Am. Chem. Soc.* **2021**, *143*, 912−924.
(9) Anderson, M.; Moshnikova, A.; Engelman, D. M.; Reshetnyak, Y. K.; Andreev, O. A. Probe for the Measurement of Cell Surface PH in Vivo and Ex Vivo. *Proc. Natl. Acad. Sci. U. S. A.* **2016**, *113*, 8177−8181.
(10) Bumpus, T. W.; Baskin, J. M. Greasing the Wheels of Lipid Biology with Chemical Tools. *Trends Biochem. Sci.* **2018**, *43*, 970−983.
(11) Flores, J.; White, B. M.; Brea, R. J.; Baskin, J. M.; Devaraj, N. K. Lipids: Chemical Tools for Their Synthesis, Modification, and Analysis. *Chem. Soc. Rev.* **2020**, *49*, 4602−4614.
(12) Harayama, T.; Riezman, H. Understanding the Diversity of Membrane Lipid Composition. *Nat. Rev. Mol. Cell Biol.* **2018**, *19*, 281−296.
(13) Holthuis, J. C. M.; Menon, A. K. Lipid Landscapes and Pipelines in Membrane Homeostasis. *Nature* **2014**, *510*, 48−57.
(14) Vance, J. E. Phospholipid Synthesis and Transport in Mammalian Cells. *Traffic* **2015**, *16*, 1−18.
(15) Tsuchiya, M.; Tachibana, N.; Nagao, K.; Tamura, T.; Hamachi, I. Organelle-Selective Click Labeling Coupled with Flow Cytometry Allows High-Throughput CRISPR Screening of Genes Involved in Phosphatidylcholine Metabolism. *bioRxiv* **2022**, 488621.
(16) Jao, C. Y.; Roth, M.; Welti, R.; Salic, A. Metabolic Labeling and Direct Imaging of Choline Phospholipids in Vivo. *Proc. Natl. Acad. Sci. U. S. A.* **2009**, *106*, 15332−15337.
(17) Jao, C. Y.; Roth, M.; Welti, R.; Salic, A. Biosynthetic Labeling and Two-Color Imaging of Phospholipids in Cells. *ChemBioChem* **2015**, *16*, 472−476.
(18) Tamura, T.; Fujisawa, A.; Tsuchiya, M.; Shen, Y.; Nagao, K.; Kawano, S.; Tamura, Y.; Endo, T.; Umeda, M.; Hamachi, I. Organelle Membrane-Specific Chemical Labeling and Dynamic Imaging in Living Cells. *Nat. Chem. Biol.* **2020**, *16*, 1361−1367.
(19) Bumpus, T. W.; Liang, F. J.; Baskin, J. M. Ex Uno Plura: Differential Labeling of Phospholipid Biosynthetic Pathways with a Single Bioorthogonal Alcohol. *Biochemistry* **2018**, *57*, 226−230.
(20) Damnjanović, J.; Iwasaki, Y. Phospholipase D as a Catalyst: Application in Phospholipid Synthesis, Molecular Structure and Protein Engineering. *J. Biosci. Bioeng.* **2013**, *116*, 271−280.
(21) Koepsell, H. Organic Cation Transporters in Health and Disease. *Pharmacol. Rev.* **2020**, *72*, 253−319.
(22) Koepsell, H. Polyspecific Organic Cation Transporters: Their Functions and Interactions with Drugs. *Trends Pharmacol. Sci.* **2004**, *25*, 375−381.
(23) Ciarimboli, G.; Struwe, K.; Arndt, P.; Gorboulev, V.; Koepsell, H.; Schlatter, E.; Hirsch, J. R. Regulation of the Human Organic Cation Transporter HOCT1. *J. Cell. Physiol.* **2004**, *201*, 420−428.
(24) Biermann, J.; Lang, D.; Gorboulev, V.; Koepsell, H.; Sindic, A.; Schröter, R.; Zvirbliene, A.; Pavenstädt, H.; Schlatter, E.; Ciarimboli, G. Characterization of Regulatory Mechanisms and States of Human Organic Cation Transporter 2. *Am. J. Physiol. Cell Physiol.* **2006**, *290*, C1521−C1531.
(25) Alamudi, S. H.; Satapathy, R.; Kim, J.; Su, D.; Ren, H.; Das, R.; Hu, L.; Alvarado-Martínez, E.; Lee, J. Y.; Hoppmann, C.; Peña-Cabrera, E.; Ha, H.-H.; Park, H.-S.; Wang, L.; Chang, Y.-T. Development of Background-Free Tame Fluorescent Probes for Intracellular Live Cell Imaging. *Nat. Commun.* **2016**, *7*, 11964.
(26) Bumpus, T. W.; Baskin, J. M. Clickable Substrate Mimics Enable Imaging of Phospholipase D Activity. *ACS Cent. Sci.* **2017**, *3*, 1070−1077.
(27) Bumpus, T. W.; Baskin, J. M. A Chemoenzymatic Strategy for Imaging Cellular Phosphatidic Acid Synthesis. *Angew. Chem., Int. Ed.* **2016**, *128*, 13349−13352.
(28) Andreev, E.; Brosseau, N.; Carmona, E.; Mes-Masson, A.-M.; Ramotar, D. The Human Organic Cation Transporter OCT1 Mediates High Affinity Uptake of the Anticancer Drug Daunorubicin. *Sci. Rep.* **2016**, *6*, 20508.
(29) Su, W.; Yeku, O.; Olepu, S.; Genna, A.; Park, J.-S.; Ren, H.; Du, G.; Gelb, M. H.; Morris, A. J.; Frohman, M. A. 5-Fluoro-2-Indolyl Des-Chlorohalopemide (FIPI), a Phospholipase D Pharmacological Inhibitor That Alters Cell Spreading and Inhibits Chemotaxis. *Mol. Pharmacol.* **2009**, *75*, 437−446.

(30) Lin, L.; Yee, S. W.; Kim, R. B.; Giacomini, K. M. SLC Transporters as Therapeutic Targets: Emerging Opportunities. *Nat. Rev. Drug Discov.* **2015**, *14*, 543−560.
(31) Perland, E.; Fredriksson, R. Classification Systems of Secondary Active Transporters. *Trends Pharmacol. Sci.* **2017**, *38*, 305−315.
(32) Hediger, M. A.; Clémençon, B.; Burrier, R. E.; Bruford, E. A. The ABCs of Membrane Transporters in Health and Disease (SLC Series): Introduction. *Mol. Asp. Med.* **2013**, *34*, 95−107.
(33) Liang, D.; Wu, K.; Tei, R.; Bumpus, T. W.; Ye, J.; Baskin, J. M. A Real-Time, Click Chemistry Imaging Approach Reveals Stimulus-Specific Subcellular Locations of Phospholipase D Activity. *Proc. Natl. Acad. Sci. U. S. A.* **2019**, *116*, 15453−15462.
(34) Du, G.; Altshuller, Y. M.; Vitale, N.; Huang, P.; Chasserot-Golaz, S.; Morris, A. J.; Bader, M.-F.; Frohman, M. A. Regulation of Phospholipase D1 Subcellular Cycling through Coordination of Multiple Membrane Association Motifs. *J. Cell Biol.* **2003**, *162*, 305−315.
(35) Flis, V. V.; Daum, G. Lipid Transport between the Endoplasmic Reticulum and Mitochondria. *Cold Spring Harbor Perspect. Biol.* **2013**, *5*, a013235.
(36) Wong, L. H.; Gatta, A. T.; Levine, T. P. Lipid Transfer Proteins: The Lipid Commute via Shuttles, Bridges and Tubes. *Nat. Rev. Mol. Cell Biol.* **2019**, *20*, 85−101.
(37) Peretti, D.; Kim, S.; Tufi, R.; Lev, S. Lipid Transfer Proteins and Membrane Contact Sites in Human Cancer. *Front. Cell Dev. Biol.* **2020**, *7*, 371.
(38) Tatsuta, T.; Scharwey, M.; Langer, T. Mitochondrial Lipid Trafficking. *Trends Cell Biol.* **2014**, *24*, 44−52.
(39) Watanabe, T.; Chuma, S.; Yamamoto, Y.; Kuramochi-Miyagawa, S.; Totoki, Y.; Toyoda, A.; Hoki, Y.; Fujiyama, A.; Shibata, T.; Sado, T.; Noce, T.; Nakano, T.; Nakatsuji, N.; Lin, H.; Sasaki, H. MITOPLD Is a Mitochondrial Protein Essential for Nuage Formation and PiRNA Biogenesis in the Mouse Germline. *Dev. Cell* **2011**, *20*, 364−375.
(40) Lin, C.; Yan, J.; Kapur, M. D.; Norris, K. L.; Hsieh, C.; Huang, D.; Vitale, N.; Lim, K.; Guan, Z.; Wang, X.; Chi, J.; Yang, W.; Yao, T. Parkin Coordinates Mitochondrial Lipid Remodeling to Execute Mitophagy. *EMBO Rep.* **2022**, No. e55191.
(41) Adachi, Y.; Itoh, K.; Yamada, T.; Cerveny, K. L.; Suzuki, T. L.; Macdonald, P.; Frohman, M. A.; Ramachandran, R.; Iijima, M.; Sesaki, H. Coincident Phosphatidic Acid Interaction Restrains Drp1 in Mitochondrial Division. *Mol. Cell* **2016**, *63*, 1034−1043.

https://doi.org/10.1021/jacsau.2c00419
JACS Au 2022, 2, 2703−2713